Carbohydrate Polymers 83 (2011) 1757–1765

Contents lists available at ScienceDirect

Carbohydrate Polymers

journal homepage: www.elsevier.com/locate/carbpol

Effect of starch fractions on spherulite formation and microstructure

Ursula V. Lay Ma, John D. Floros, Gregory R. Ziegler*

Department of Food Science, The Pennsylvania State University, 341 Food Science Building, University Park, PA 16802, United States

ARTICLE INFO

Article history:
Received 5 August 2010
Received in revised form 18 October 2010
Accepted 19 October 2010
Available online 27 October 2010

Keywords:
Starch fractions
Spherulites
Microstructure

ABSTRACT

The effect of amylose, amylopectin, and intermediate material on starch spherulite formation and microstructure was investigated. Spherulites were observed in all samples made from high amylose maize starch fractions, but could not be observed when common corn or potato amylopectin were used. More numerous and better developed spherulites were formed with higher proportions of amylose. The dissolution temperature of spherulites made from common corn and potato starch amylose was 123–124 °C and 110–111 °C, respectively. However, the dissolution temperature of spherulites made from high amylose maize starch fractions decreased with higher proportions of branched material, ranging from 93 °C to 116 °C. SEM, TEM, and AFM images showed that starch spherulites may develop from a sheaf-like precursor, have an internal radial organization, and a blocklet nanostructure similar to some synthetic spherulites. This study shows that spherulitic crystallization of starch is favored by a higher ratio of linear to branched material.

1. Introduction

Spherulites have been described as approximately radially symmetric semicrystalline structures formed by crystal lamellae or fibers. When these structures are viewed between cross polarizers, they exhibit a characteristic "Maltese cross" extinction pattern (Creek, Ziegler, & Runt, 2006). Two types of spherulitic crystallization from native starches have been reported. In one case, spherulitic crystallization is induced by the formation of amylose inclusion complexes with fatty acids. To obtain this type of spherulite, an aqueous starch dispersion is heated to 140 °C in the presence of lipids, followed by slow cooling (Fanta, Felker, & Shogren, 2002; Fanta, Felker, Shogren, Byars, & Salch, 2005; Fanta, Felker, Shogren, & Salch, 2006; Peterson, Fanta, Adlof, & Felker, 2005; Shogren, Fanta, & Felker, 2006). The second type of spherulite is formed when an aqueous starch dispersion is heated above 170 °C followed by rapid cooling (Nordmark & Ziegler, 2002a, 2002b; Ziegler, Creek, & Runt, 2005; Ziegler, Nordmark, & Woodling, 2003). The formation of these latter particles does not require the presence of amylose inclusion complexes (Nordmark & Ziegler, 2002a) and is the focus of this article.

Ziegler et al. (2003) reported that a heat treatment above 170 °C and fast cooling were necessary for the formation of well developed spherulites. Creek et al. (2006) hypothesized that this temperature was necessary to go through a helix → coil transition in order to avoid gel formation during cooling caused by the presence of helical nuclei. These authors proposed that during heating, when the dispersion reaches around 70 °C, double helical crystallites begin to "dissolve," and by 130 °C thermal dissociation of fixed network entanglements occurs to form a liquid-crystalline phase. Then between 160 °C and 180 °C the solution becomes isotropic, which is necessary for spherulite formation upon cooling (Creek et al., 2006). More recently, Nishiyama, Putaux, Montesanti, Hazemann, & Rochas (2010) observed a B → A transition at approximately 120 °C when amylose "spherocrystals" were heated in excess water. This was followed by melting of the A type crystals at 160 °C. During cooling, phase separation is induced, resulting in a polymer-poor phase, and a polymer-rich phase in which spherulitic crystallization occurs. At slow cooling rates, crystallization can occur before phase separation, which may result in network formation preventing demixing (Ziegler et al., 2005).

Some structural features reported for spherulites made from high amylose maize starches (*ae* 70) are a radially oriented structure, and the presence of a central cavity and small holes away from the center (Nordmark & Ziegler, 2002b). Creek (2007) also suggested a radially oriented layered structure for spherulites made from common corn amylose with varying degrees of polymerization (DP). Atomic force microscopy (AFM) images of the interior of spherulites have shown the presence of blocklets of 20–60 nm (Creek, 2007; Suwanayuen, 2009) similar in appearance to blocklets observed in granular starches (Creek, 2007; Sujka & Jamroz, 2009).

Spherulite formation depends on the starch source (Ziegler et al., 2003). Nordmark and Ziegler (2002) studied the spherulitic crystallization of high amylose maize starch (*ae* 50 and *ae* 70), common corn starch (CCS), waxy maize starch, amylose from high amylose

* Corresponding author. Tel.: +1 814 863 2960; fax: +1 814 863 6132.
E-mail address: grz1@psu.edu (G.R. Ziegler).

0144-8617/$ – see front matter © 2010 Elsevier Ltd. All rights reserved.
doi:10.1016/j.carbpol.2010.10.041

maize starch (*ae* 70), and amylopectin from waxy maize starch. These authors reported that spherulite formation is favored by linear material (amylose) and that spherulites were practically absent in amylopectin samples (waxy maize). Similarly, Creek et al. (2006) reported that amylopectin from potato starch did not form spherulites when heating a 10% dispersion to 180 °C and cooling to 10 °C at cooling rates varying from 1 to 250 °C/min.

Klucinec and Thompson (1998) separated high-amylose maize starches into three fractions – amylose, amylopectin and intermediate material – using differential alcohol precipitation and then characterized these fractions chromatographically and by iodine binding. They determined that the so-called intermediate material had a blue value and iodine binding wavelength maximum between those of the amylose and amylopectin fractions. Chain length distributions of amylopectin and intermediate material showed that while both were branched, the average chain length of the intermediate material was greater. They concluded that the differential precipitation behavior resulted from the branching structure. Nordmark and Ziegler (2002a) suggested that this branching structure of intermediate material may be ideal for spherulite formation.

However, no attempts have been made previously to investigate this hypothesis, and the effect of various proportions of starch fractions (amylose, amylopectin, and intermediate material) isolated from a single source and then recombined on spherulite formation and microstructure has not been studied in a systematic manner. The objective of this study was to investigate the effect of amylose, amylopectin, and intermediate material obtained from common corn starch, high amylose maize starch, and potato starch, on spherulite formation and its microstructure.

2. Materials and methods

2.1. Materials

High amylose maize starch (Hylon VII) and CCS were supplied by National Starch and Chemical Company (Bridgewater, NJ, USA). Potato amylose from Sigma–Aldrich Inc. (St. Louis, MO, USA) and potato amylopectin from Fluka Chemie (Buchs, Switzerland) were used. Dimethyl sulfoxide (DMSO), isoamyl alcohol and 1-butanol were obtained from Sigma–Aldrich Inc. (St. Louis, MO, USA).

2.2. Starch fractionation

Starch fractions, amylose, amylopectin, and intermediate material from Hylon VII and CCS, were obtained by differential alcohol precipitation using isoamyl alcohol and 1-butanol as described by Klucinec and Thompson (1998).

2.3. Sample preparation

Starch spherulites with various proportions of amylose, amylopectin and intermediate material from Hylon VII and CCS were prepared following a simple lattice mixture design with a degree of lattice of 3 and one center point. Starch spherulites with various proportions of potato amylose and potato amylopectin were also prepared (100:0, 80:20, 60:40, 40:60, 20:80, and 0:100). Spherulites were produced in a differential scanning calorimeter (DSC-7, Perkin-Elmer Instruments, Norwalk, CT, USA). Starch fractions were weighed in 60 μL stainless steel DSC pans, and water was added to obtain a 10% (w/w) dispersion. Pans were hermetically sealed and kept overnight at room temperature for moisture equilibration. Samples were heated from 20 °C to 180 °C at a rate of 10 °C/min, and immediately cooled to 10 °C at a rate of 25 °C/min. Samples were stored overnight in the sealed pans before further analysis.

2.4. Microscopy

Immediately after opening the pans using a pair of pliers, samples were mixed using a micro-spatula, and a small aliquot was observed using a BX41 light microscope equipped with polarizing filters (Olympus, Edgemont, PA, USA) connected to a digital camera (Spot Insight QE camera, Diagnostic Instruments Inc., Sterling Heights, MI, USA). The remaining sample in the DSC pans were washed with water, then with ethanol, dried at room temperature, and stored in a desiccator until further analysis.

For scanning electron microscopy (SEM), dried samples were fractured using a mortar and pestle to separate aggregates formed during drying. A thin layer of sample was placed on aluminum stubs with conductive carbon tape and sputter coated with gold. Samples were observed using an environmental scanning electron microscope (Quanta 200 ESEM, FEI Company, Hillsboro, OR, USA) under low vacuum mode of 0.68 Torr and voltage of 15 kV.

For transmission electron microscopy (TEM), samples were stained using the periodic acid thiosemicarbazide silver method as described by Planchot, Colonna, Gallant, & Bouchet (1995). With this method, samples are stained before embedding, so staining after sectioning is not necessary. By this method, the starch is oxidized to a low degree, and the silver ions react preferentially with the amorphous regions, which appear dark in the TEM images (Gallant, Bouchet, & Baldwin, 1997). To ensure a more homogeneous distribution of the sample and avoid losing material during sample preparation, dried samples were collected in a microcentrifuge tube and mixed with 50 μL of a 3% (w/v) agar solution at 45 °C. The agar was solidified at room temperature, and then broken into small pieces using a needle. Samples were treated with 1 mL of a 1% periodic acid solution for 30 min at room temperature followed by centrifugation. The precipitate was washed three times with deionized water. Samples were then treated with 1 mL of a supersaturated solution of semithiocarbazide for 24 h. The semithiocarbazide solution was removed and 1 mL of a 1% silver nitrate aqueous solution was added. Samples were kept in this solution for 4 days in dark conditions. Samples were washed three times with deionized water, followed by dehydration by a series of 50%, 70%, 90%, and 100% aqueous ethanol. Samples were treated with 1 mL of each ethanol solution for 5 min, then washed three times with electron microscopy grade ethanol for 5 min, and three times with acetone for 5 min. Samples were infiltrated in a 50/50 eponate resin/acetone mixture for 7 h, and then in a 75/25 eponate resin/acetone mixture for another 7 h. After infiltration, samples were embedded in 100% eponate resin for 7 h followed by resin polymerization at 60 °C for 16 h (Evans, 2002). Thin sections (70–90 nm) of the embedded samples were obtained and observed using a JEOL 1200 EXII TEM (Peabody, MA, USA). Thick sections (200 nm) were collected on a glass slide and stained with toluidine blue and viewed using a light microscope. Thick sections (500 nm) were obtained for AFM.

AFM was performed on a Digital Dimension 3100 atomic force microscope (Veeco Instruments, Wodbury, NY, USA) in tapping mode. Images were analyzed using the WSxM Scanning Probe Microscopy Software (4.0 v.12.6 2008, Nanotec Electronica S. L., Madrid, Spain). Roughness of the central and outer regions of the spherulites was determined from 0.5 μm × 0.5 μm images of at least two spherulites using the roughness analysis tool of the WSxM software, and reported as roughness root mean square (RMS). The width and height of the outer region of at least 5 spherulites per sample were measured using the profile tool of the WSxM software. Three different line profile curves were generated for each spherulite. For each profile, two measurements of the width and height of the outer region were obtained. Blocklet size was also measured using the profile tool. For blocklet size, three line profile curves were generated (one horizontal and two diagonal lines)

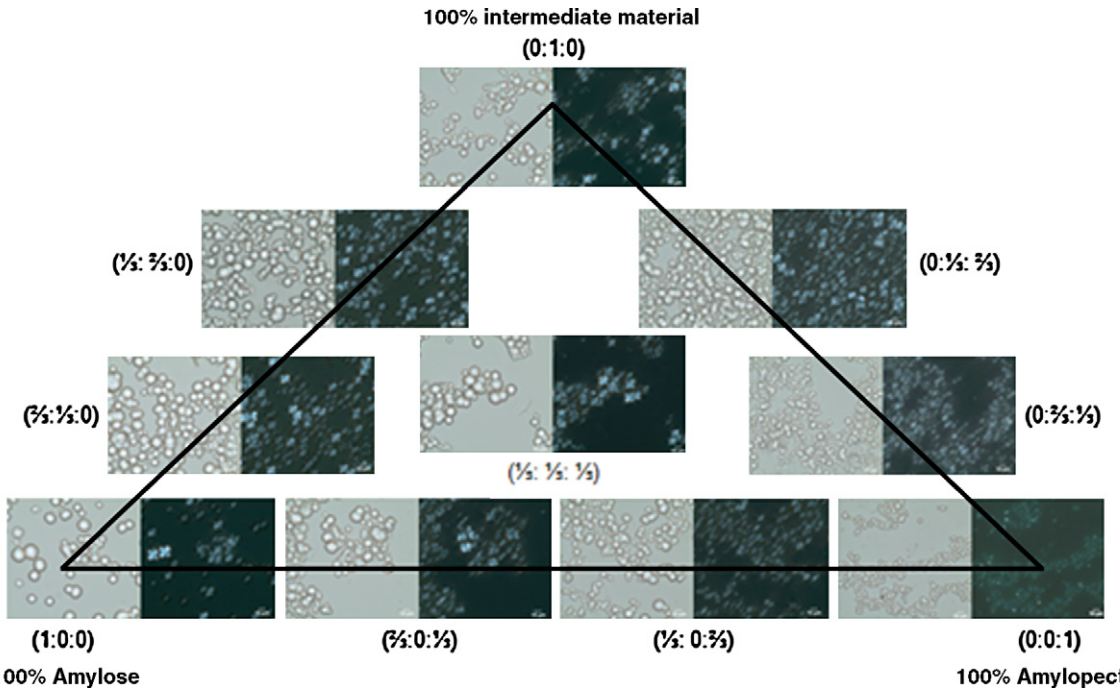

Fig. 1. Morphology of spherulites made with various proportions of Hylon VII fractions observed under brightfield (left) and polarized (right) illumination. Numbers in parentheses show the proportion of amylose:intermediate material:amylopectin based on the mixture design. Scale bars = 10 μm.

from at least two images per region (central and outer region) and all blocklets of each profile curve were measured. The average of at least 60 blocklets per region was reported for each sample.

2.5. Thermal analysis

After storing overnight in the sealed pans, samples were heated in a Thermal Advantage Q100 DSC (TA Instruments, New Castle, DE, USA) to 180 °C at 10 °C/min. The DSC was calibrated with indium, and an empty sample pan was used as a reference. The baseline was obtained by processing two empty pans using the same heating treatment and subtracted from the data. Data were analyzed using the TA Universal Analysis software (Universal Analysis 2000 v.4.2E, TA Instruments-Waters LLC, New Castle, DE, USA).

2.6. Statistical analysis

The mixture design was analyzed using the general regression model tool of Statistica 6.1 software (StatSoft Inc., Tulsa, OK, USA). Multiple comparisons of roughness, blocklet size, outer region width and height of starch spherulites made from Hylon VII amylose, amylopectin, and intermediate material were performed using the "Proc GLM" and "means" procedures and Tukey test for multiple comparisons of SAS 9.1 for Windows (SAS Institute Inc., Cary, NC, USA).

3. Results and discussion

3.1. Microscopy

All treatments containing Hylon VII amylose, amylopectin or intermediate material formed spherulites with the characteristic Maltese cross when observed between cross polarizers (Fig. 1). Spherulites could not be observed in samples made of CCS amylopectin and potato amylopectin. Instead, a few small birefringent but non-spherulitic particles were observed (data not shown). However, spherulites were formed in all samples containing at least 33% CCS amylose or intermediate material, or 20% potato amylose. Previous studies have also reported that waxy maize (i.e. amylopectin) (Nordmark & Ziegler, 2002a) and potato amylopectin (Creek et al., 2006) did not form spherulites. The longer chains of amylopectin from Hylon VII starch [average chain length 48.5 DP (Klucinec & Thompson, 2002)] as compared to the chains of waxy maize [average chain length 23–24 DP (Hizukuri, 1985; Klucinec & Thompson, 2002)], common corn [average chain length 26–28 DP (Hizukuri, 1985; Klucinec & Thompson, 2002)] and potato amylopectin [average chain length 34 DP (Hizukuri, 1985)] could be responsible for the observed difference. Other factors such as chain length distribution or degree of branching may also be responsible for spherulitic crystallization of Hylon VII amylopectin. For example, Hylon VII amylopectin has a higher proportion of longer to shorter chains as compared to common corn, waxy corn, and potato amylopectin (Hizukuri, 1985).

Larger amounts of non-spherulitic material and less rounded spherulites were observed as the proportion of branched material increased, consistent with previous observations by Nordmark and Ziegler (2002a). Linear chains, such as amylose, would be expected to fold more easily to form the crystalline lamellae (Nordmark & Ziegler, 2002a). The reduced extent of spherulitic crystallization caused by higher concentration of branches has also been reported for synthetic polymers (Chowdhury, Haigh, Mandelkern, & Alamo, 1998; Jayakannan & Ramakrishnan, 1999).

Various microscopy techniques were used to observe the internal structure of starch spherulites. The characteristic internal radial organization could be observed (Fig. 2). Nordmark and Ziegler (2002b) reported the presence of a central cavity in Hylon VII spherulites. However, this cavity was not observed in TEM and AFM images of cross-sections of spherulites. It may be possible that the cross-sections were not from a region close to the center of the spherulites and for that reason the central cavity was not observed. To eliminate this possibility, cross sections from various depths of the resin blocks containing the spherulites were obtained and evaluated under the light microscope. The central cavity was not observed in these cross-sections.

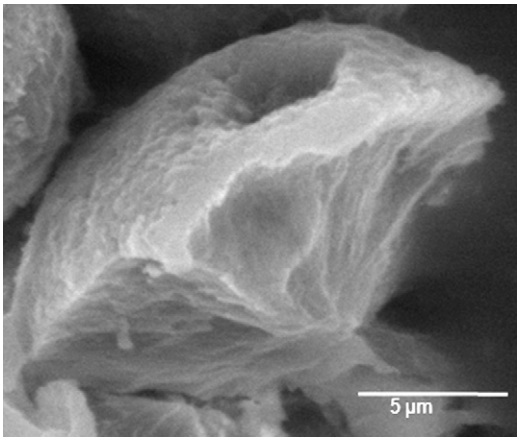

Fig. 2. SEM image of broken spherulites made from 100% amylose from Hylon VII showing the internal radial organization.

TEM images of intermediate material and amylopectin spherulites showed small holes away from the center, which were more numerous and larger in amylopectin spherulites (Fig. 3). These holes may provide higher amylase accessibility to the interior of these spherulites probably increasing their susceptibility to enzyme hydrolysis. On the other hand, the more dense structure of amylose spherulites may provide less access to the interior of the spherulite resulting in higher resistance to amylase hydrolysis. Images of cross-sections of spherulites showed that starch spherulites may develop from a sheaf-like precursor (shown with white arrows in Fig. 3) similar to the spherulitic crystallization model for synthetic polymers (Bassett & Keith, 1984; Granasy, 2006; Granasy, Pusztai, Tegze, Warren, & Douglas, 2005; Khoury & Passaglia, 1976; Li et al., 2000; Phillips, 1994). In several TEM images of amylose, intermediate material, and amylopectin spherulites, a darker external region was observed, similar to that observed in the 100% amylose spherulite in Fig. 3.

As explained in the microscopy section of materials and methods, silver ions react preferentially with amorphous regions resulting in a darker appearance in TEM images. Therefore, the proportion of amorphous material towards the outside of the spherulites was higher than in the center. On the other hand, the lighter central region indicates a larger amount of crystalline material in the center of the spherulite.

Cross-sections of spherulites made of amylose, intermediate material, amylopectin from Hylon VII had similar AFM topographic images. These images showed a darker central region and a brighter periphery (Fig. 4a), which indicates that the periphery of the cross-sections of spherulites had taller features. A similar observation was reported by Ridout, Parker, Hedley, Bogracheva, & Morris (2004) for granules of wild-type pea starch. These authors explained that during sectioning, the granule was exposed, absorbed water and swelled. When the section subsequently dried out, the central region collapsed more than the periphery. To corroborate this, Ridout et al. (2004) encased dry starch granules in a drop of a rapid-set Araldite. Once the drop was set, the top surface was cut to produce a flat surface with starch granules with cut faces exposed. AFM images of the dried cut faces of encased granules were featureless, but after exposing them to water, images showed a large height variation between the periphery and central region, which was not reversible after drying the wetted blocks for three months in a desiccator over P_2O_5. These authors hypothesized that the difference in height between the central and outer region originated due to a difference in structure with different swelling behavior.

Similarly, it is possible that the structure of the center and the periphery of the spherulites in our study were different, resulting in a difference in swelling after sectioning of samples. As described above, TEM images showed a darker outer region sug-

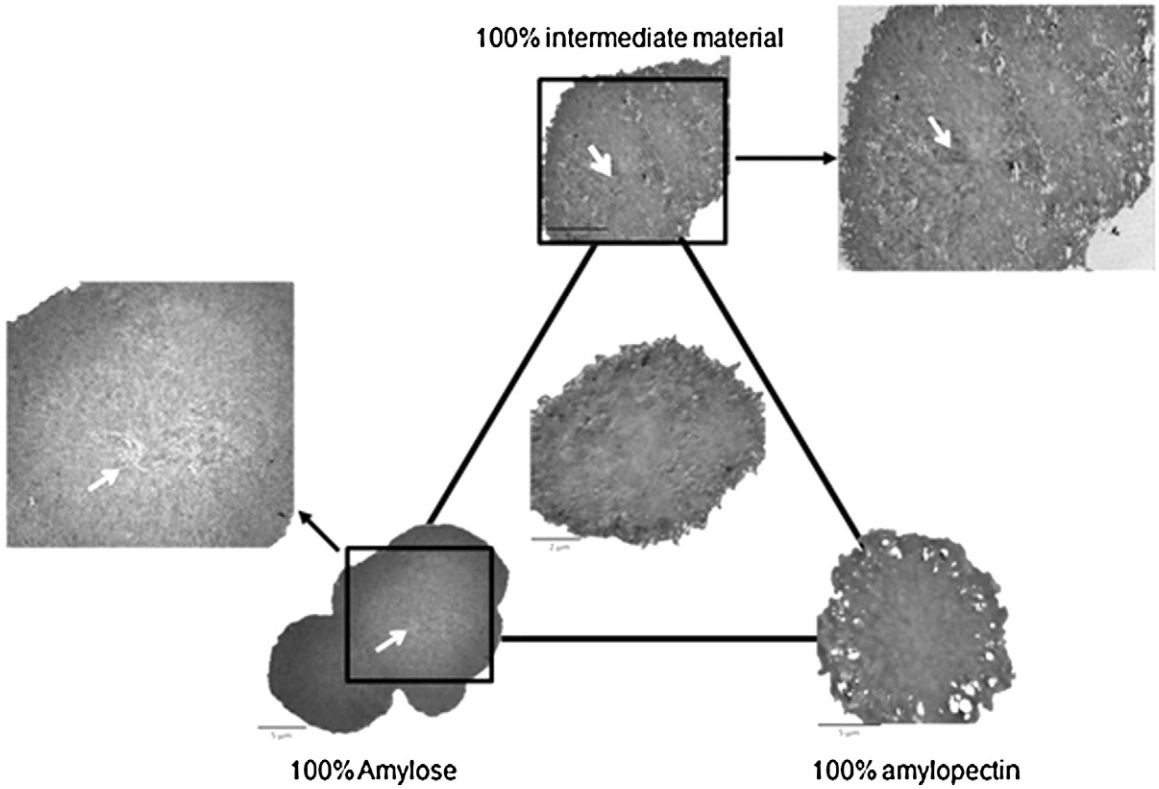

Fig. 3. TEM images of cross sections of spherulites made with various proportions of Hylon VII amylose, intermediate material, and amylopectin. White arrows show a sheaf-like structure.

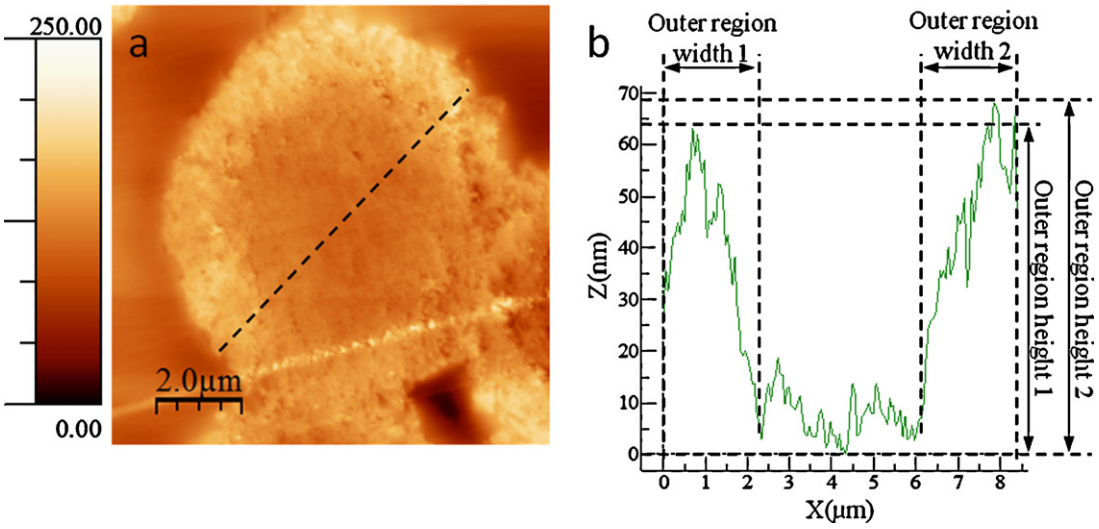

Fig. 4. AFM topographic image of a spherulite made from Hylon VII amylopectin (a) and line profile (b) of the dashed line on topographic image showing the width and height measurements of the outer region of spherulites. Relative set point = 0.8. Scan size 10 μm × 10 μm.

gesting a higher proportion of amorphous material, which would swell preferentially upon water exposure. The average width of the darker outer region of spherulites observed in TEM images made from Hylon VII amylose, intermediate material, and amylopectin was 2.7 ± 0.8 μm, 2.0 ± 0.2 μm, and 1.8 ± 0.2 μm, respectively. This width was similar to the width of the taller outer region observed in AFM images (Table 1) supporting the idea of preferential swelling of the outer more amorphous region of the spherulite.

The extent and height of the outer region with taller features varied depending on the starch fraction. Amylose spherulites had a wider region with taller features compared to amylopectin and intermediate material spherulites (Table 1). It is possible that the difference in the proportion of amorphous material between the outer and central regions of amylose spherulites was larger than that of their amylopectin counterparts, which resulted in higher water absorption and swelling. It is also possible that the branch structure of amylopectin holding the clusters together, limited the absorption of water and swelling during sectioning of samples. Klucinec and Thompson (1998) reported that the structure of the intermediate material of Hylon VII starch is more similar to amylopectin than to amylose, and therefore, a similar swelling behavior of spherulites made of intermediate material and amylopectin is not surprising.

Despite the difference in height between the center and the edges of the spherulites, both regions showed a granular structure (Fig. 5) due to the presence of blocklets of approximately 19–26 nm (Table 1). In general, the outer region showed a rougher surface than the central region, which was to be expected if the outer region had swollen giving rise to taller protuberances. No significant differences in roughness were observed among spherulites made of different starch fractions ($\alpha = 0.05$) (Table 1). The blocklet structure could be identified in both topographic and phase images. The presence of 20–60 nm blocklets have also been reported in spherulites made from corn amylose with various DP (Creek, 2007; Suwanayuen, 2009). Blocklets of 20–500 nm in size have also been observed in starch granules from various botanical sources (Baker, Miles, & Helbert, 2001; Gallant et al., 1997; Ohtani, Yoshino, Hagiwara, & Maekawa, 2000; Ridout, Parker, Hedley, Bogracheva, & Morris, 2003; Ridout et al., 2004; Ridout, Parker, Hedley, Bogracheva, & Morris, 2006; Sujka & Jamroz, 2009; Szymonska & Krok, 2003). In starch granules, blocklets are believed to be formed by amylopectin side chains (Gallant et al., 1997), while in spherulites, blocklets are said to be formed by amylose (Creek, 2007).

The granular appearance has also been observed in spherulites made of synthetic polymers. Ivanov and Magonov (2003) proposed that the granular structure of low density polyethylene (LDPE) spherulites observed in topographic images was caused by amorphous regions of polymer chains on the surfaces of the crystalline lamellae (Ivanov & Magonov, 2003). By increasing the tip-sample force, these authors showed a fibril structure instead of a granular appearance suggesting that fibrils and lamellae were formed by a crystalline core. However, in the present investigation, the granular appearance persisted when the tip-sample force was doubled. Higher sample tip force could cause damage to the surface of the sample or the tip itself. It could be possible that the tip sample force was not high enough to go through the amorphous patches of starch, and therefore, the granular appearance remained. However, phase images (Fig. 5b) contradicted the idea that the granular appearance is caused by the amorphous patches described by Ivanov and Magonov (2003). In phase images, the lighter color represents harder regions and darker color softer regions. The brighter color of the blocklets surrounded by darker regions suggests that blocklets were composed of more crystalline regions surrounded by

Table 1
Roughness, blocklet size, wall thickness and height of starch spherulites made from different Hylon VII starch fractions (mean ± standard deviation).[a]

Material	RMS roughness[b,c]		Blocklet size[b,c] (nm)		Outer region width[b] (μm)	Outer region height[b] (nm)
	Outer region	Central region	Outer region	Central region		
Amylose	3.9 ± 0.3aA	3.4 ± 0.1aB	20 ± 7aA	19 ± 7aA	2.8 ± 0.7a	74 ± 23a
Intermediate material	4.6 ± 0.1aA	3.2 ± 0.3aB	23 ± 8bA	25 ± 10bA	2.1 ± 0.2b	54 ± 6b
Amylopectin	4.7 ± 0.8aA	3.8 ± 1.5aA	26 ± 9bA	23 ± 8bA	1.9 ± 0.2b	54 ± ±9b

[a] RMS roughness and blocklet size were measured from 0.5 × 0.5 μm images.
[b] Same lower case letters within column indicate no significant differences at $\alpha = 0.05$.
[c] Same upper case letters within the same material (row) indicate no significant differences ($\alpha = 0.05$) in roughness or blocklet size between the outer and central region.

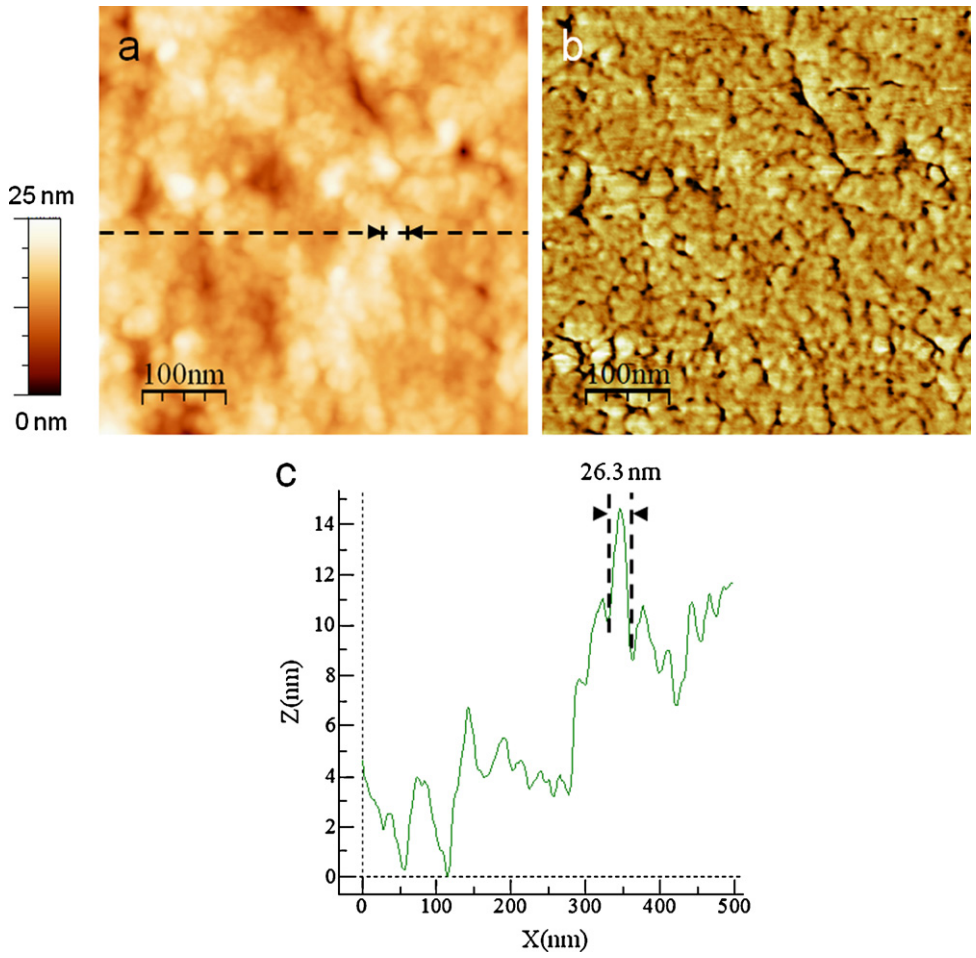

Fig. 5. AFM topographic (a) and phase (b) images of the central region of a Hylon VII amylose spherulite (c) represents the line profile of the dashed line on image (a) showing the measurement of the size of one blocklet. Relative set point = 0.8. Scan size 0.5 μm × 0.5 μm.

amorphous material. It is also possible that during sample preparation, the resin or the agar infiltrated inside the spherulites, and the observed granular structure represents crystalline or semicrystalline blocklets surrounded by the infiltrated resin or agar.

Strobl (2006) hypothesized that during crystallization of synthetic polymers, a transient intermediate 'granular' stage occurs as the crystalline lamellae is developed. The crystalline units from the 'granular' stage will merge to form the complete crystalline lamellae given sufficient time for their formation (Strobl, 2000). However, the intermediate 'granular' stage may be preserved if the mobility of the crystalline segments is limited, for example by quickly cooling the polymer below Tg or by the structure of the crystalline units, such as a stable packing of helices forming the crystalline units (Creek, 2007).

If we considered that the central region of the spherulite is the region where the spherulite originated, then the crystalline units initially formed in the central area may have started coming into proximity to form the crystal lamella. Then, less amorphous material may be surrounding the blocklets, and therefore swelling may be limited. On the other hand, in the outer region, crystal units may be surrounded by more amorphous material that can absorb water and swell during sample preparation giving rise to the observed taller features of the outer region of spherulites (Fig. 4).

No significant differences ($\alpha = 0.05$) were observed between the size of the blocklets of the central and outer regions of spherulites made of the same starch fraction (Table 1). However, blocklet size varied depending on the starch fraction. Smaller blocklets were observed in amylose spherulites, and no significant size differences ($\alpha = 0.05$) were observed between the blocklets of amylopectin and intermediate material (Table 1). In granular starches, blocklets are believed to be formed by a group of clusters of amylopectin side chains (Gallant et al., 1997). These clusters have an average diameter of 9–10 nm (Gallant et al., 1997; Jenkins, Cameron, & Donald, 1993; Jenkins & Donald, 1995) and are composed of a crystalline region with double helices and an amorphous region containing the branch points (Gallant et al., 1997). The average cluster size is independent of the botanical source (Jenkins et al., 1993; Jenkins & Donald, 1995), but the size of the crystalline region within a cluster varies among starches. For example, amylomaize starch clusters have a larger crystalline region as compared to those from normal maize starch (Jenkins & Donald, 1995). If blocklets of amylopectin spherulites (20 nm approximately) were also formed by a group of these clusters like in granular starches, then amylopectin spherulite blocklets may be formed by two clusters of amylopectin side chains.

A section of Hylon VII amylose spherulites was treated with HCl 2 N for 1 h to remove the amorphous and less crystalline part of sectioned spherulites. AFM images of the acid treated spherulites (Fig. 6) showed larger blocklets than their non-acid treated counterparts (Fig. 3). Some of these larger blocklets appeared to be formed by a stack of layers (see white ovals in Fig. 6b) with an average thickness of 17.6 ± 5.0 nm. Coincidently, this thickness was not significantly different ($p > 0.05$) than the blocklet size of amylose spherulites before acid treatment (Table 1). It is possible that these layers represent crystalline lamella that stack together forming larger blocklets.

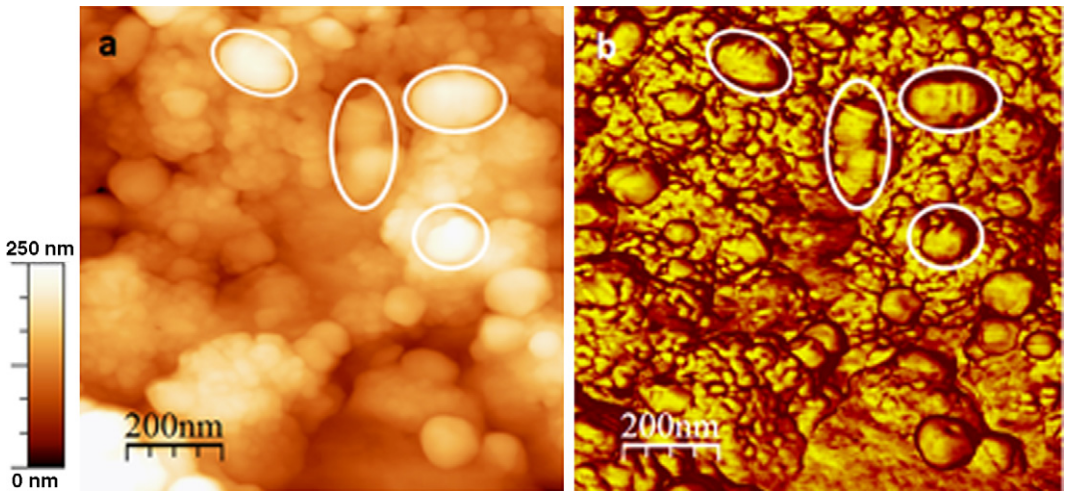

Fig. 6. AFM topographic (a) and phase (b) images of the outer region of a Hylon VII amylose spherulite treated with 2 N HCl for 1 h. Relative set point = 0.8. Scan size 1 μm × 1 μm. White ovals show the formation of layered structures.

3.2. Thermal characterization

An endothermic transition was observed in all samples made of Hylon VII fractions and can be attributed to the dissolution of spherulites. Regression analysis showed that the proportion of amylose, intermediate material, and amylopectin had a significant effect ($\alpha = 0.05$) on the onset and peak dissolution temperature, and the dissolution temperature range and enthalpy. The peak dissolution temperature increased with amylose concentration and decreased with amylopectin content (Fig. 7b). Chowdhury

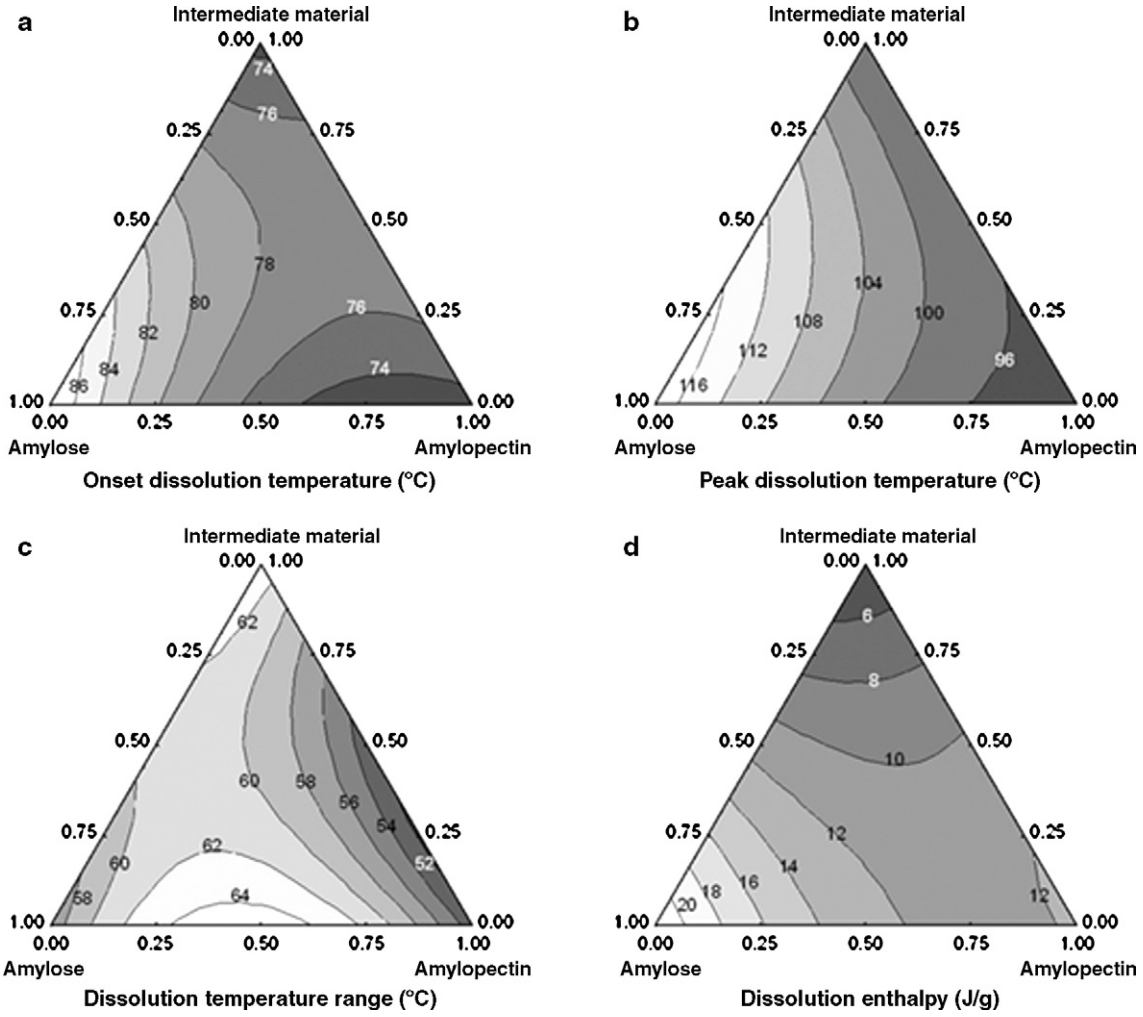

Fig. 7. Thermal characterization of starch spherulites made with various proportions of amylose, amylopectin, and intermediate material from Hylon HVII: (a) dissolution onset temperature, (b) dissolution peak temperature, (c) dissolution temperature range, and (d) dissolution enthalpy.

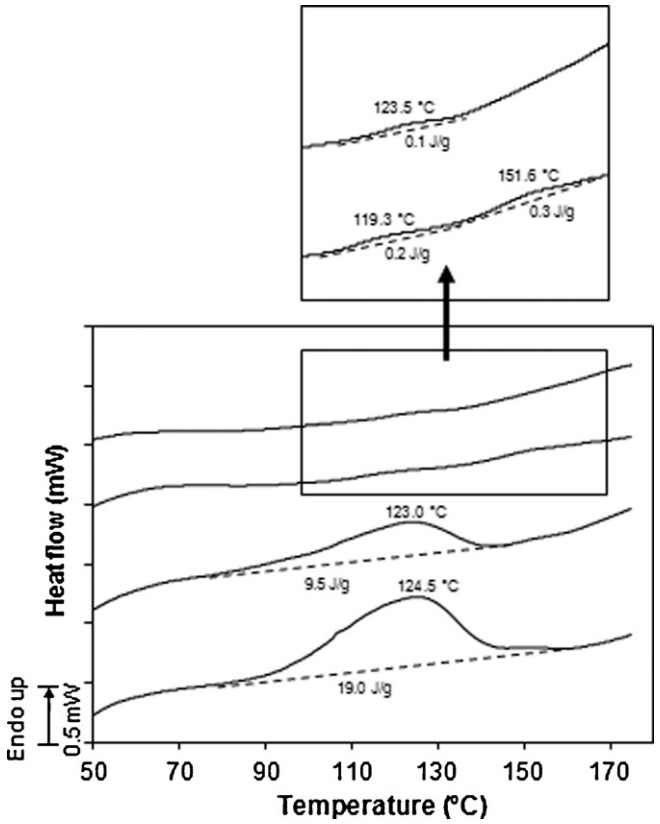

Fig. 8. Dissolution endotherm of spherulites made with various proportions of common corn amylose and amylopectin. %amylose/%amylopectin from bottom to top: 100/0, 67.7/33.3, 33.3/67.7, and 0/100.

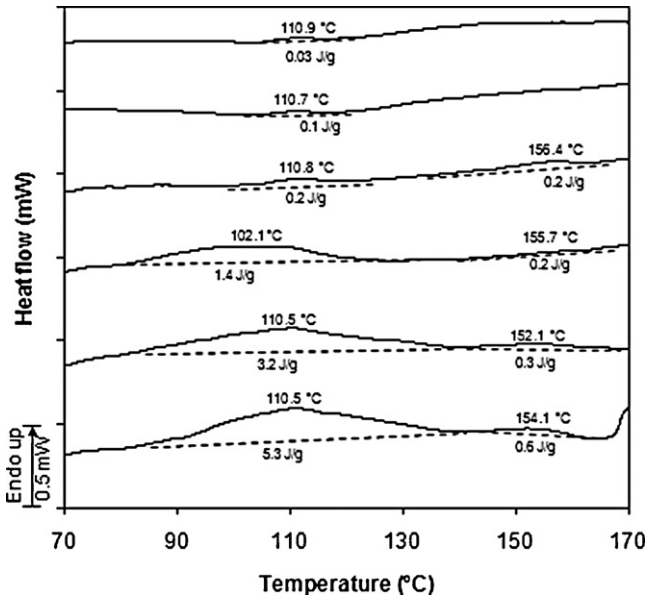

Fig. 9. Dissolution endotherm of spherulites made with various proportions of potato amylose and amylopectin. %amylose/%amylopectin from bottom to top: 100/0, 80/20, 60/40, 40/60, 20/80, and 0/100.

et al. (1998) also reported that the melting temperature of LDPE spherulites decreased with higher concentration of branch points. The longer amylose chains, as compared to intermediate material and amylopectin chains, may allow the formation of longer helices with a more heat stable conformation and thus, a higher dissolution temperature. The shorter chains of amylopectin as compared to those of intermediate material (Klucinec & Thompson, 1998) resulted in the formation of shorter helices with lower thermal stability, and thus, a lower dissolution temperature.

The range of dissolution temperature was also affected by the proportion and type of material (Fig. 7c). A larger dissolution range indicates a higher polydispersity of lamella sizes. The narrowest dissociation temperature range was observed for amylopectin spherulites. If the cluster model of the amylopectin molecule is considered, then the length and packing of double helices would probably be more uniform. The largest dissociation temperature range was observed for samples made of intermediate material, and samples made of amylose/amylopectin mixtures. It would be expected that the large differences between amylose and amylopectin molecules may result in large diversity of helical sizes. The structure of the intermediate material is not well understood. Baba and Arai (1984) suggested that the intermediate material consists in four or five branches of around 50 DP linked to a main 100–150 DP linear chain. Based on the similar chain length distribution, Klucinec and Thompson (1998) suggested that the gross branching structure is similar to that of amylopectin but with some structural differences. It is possible that the structure of the intermediate material does not follow the cluster model and a wide variety of helical lengths are formed resulting in a wide range of dissolution temperature.

The dissolution enthalpy increased with amylose content suggesting a higher degree of crystallinity for samples made with higher proportions of amylose. This observation is consistent with the greater number of spherulites and lesser amount of non-spherulitic material observed at higher amylose concentrations. However, in samples made with various proportions of amylopectin and intermediate material, the dissolution enthalpy increased at higher amylopectin concentrations, even though fewer spherulites were observed. For these samples, the onset temperature of the observed endotherms was between 71 °C and 74 °C (Fig. 7a). It is possible that the endotherm does not only represent the dissolution of spherulites, but also the dissolution of retrograded non-spherulitic amylopectin.

Spherulites made from CCS and potato starch fractions showed a dissolution endotherm at around 123–124 °C, and around 110–111 °C, respectively (Figs. 8 and 9). The dissolution peak temperature of these spherulites did not decrease with higher proportions of amylopectin, suggesting that in common corn and potato starch spherulites, amylopectin does not co-crystallize with amylose to form the spherulites. Similar to spherulites from Hylon VII fractions, the enthalpy of spherulite dissolution decreased as the ratio of amylose to amylopectin decreased (Figs. 8 and 9). This observation is consistent with the fewer spherulites observed at lower amylose concentrations. In samples containing potato amylose, a second endotherm was observed at around 155 °C, possibly representing the melting of retrograded non-spherulitic amylose (Fig. 9). This second endotherm attributed to the dissolution of retrograded non-spherulitic amylose was also observed in few common corn starch samples as shown in the insert in Fig. 8. The small endotherm observed in 100% common corn or potato amylopectin samples may be due to the dissolution of the small birefringent particles observed in these samples.

4. Conclusions

Spherulitic crystallization of starch fractions and their mixtures is greatly affected by the proportion and structure of each starch fraction. Higher ratios of linear to branched molecules resulted in the formation of more numerous and rounder spherulites with higher thermal stability. In addition to the presence of branches, it appears that spherulitic crystallization is also affected by other fac-

tors, such as degree of branching, chain length, and chain length distribution. Starch spherulites may develop from a sheaf-like precursor, and have an internal radial organization and blocklet structure similar to some synthetic spherulites. Because the ratio of amylose to amylopectin and the molecular structure of the starch fractions can affect the spherulitic crystallization of starch, these factors should be taken into account when selecting a starch source for spherulite formation.

The present investigation showed that the molecular structure and proportion of starch fractions can affect the formation of spherulites, their internal structure, and thermal properties. However, further research is needed to better understand the spherulitic crystallization of starch molecules and the internal structure of starch spherulites.

Acknowledgements

This work was funded through The Pennsylvania Agricultural Experiment Station administered by The College of Agricultural Sciences of The Pennsylvania State University. The assistance of Missy Hazen from The Huck Institutes of the Life Sciences with the TEM, and the assistance of Dr. Thomas Daniel from the Material Research Institute at the Pennsylvania State University with the AFM is also gratefully acknowledged.

References

Baba, T., & Arai, Y. (1984). Structural characterization of amylopectin and intermediate material in amylomaize starch granules. *Agricultural and Biological Chemistry*, *48*(7), 1763–1775.

Baker, A. A., Miles, M. J., & Helbert, W. (2001). Internal structure of the starch granule revealed by AFM. *Carbohydrate Research*, *330*(2), 249–256, doi:10.1016/S0008-6215(00)00275-5.

Bassett, D. C., & Keith, H. D. (1984). Electron microscopy and spherulitic organization in polymers. *Critical Reviews in Solid State and Materials Sciences*, *12*(2), 97–163, doi:10.1080/01611598408244067.

Chowdhury, F., Haigh, J. A., Mandelkern, L., & Alamo, R. G. (1998). The supermolecular structure of ethylene–vinyl acetate copolymers. *Polymer Buletin*, *41*, 463–470, doi:10.1007/s002890050388.

Creek, J. A. (2007). Nanoscale self-assembly of starch: Phase relations, formation, and structure. *Materials science and engineering* [Dissertation] (p. 235). University Park, The Pennsylvania State University.

Creek, J. A., Ziegler, G. R., & Runt, J. (2006). Amylose crystallization from concentrated aqueous solution. *Biomacromolecules*, *7*(3), 761–770, doi:10.1021/bm050766x.

Evans, A. (2002). Resistant starch from four native high-amylose maize starches. *Food science* [MSc Thesis] (p. 136). University Park, The Pennsylvania State University.

Fanta, G. F., Felker, F. C., & Shogren, R. L. (2002). Formation of crystalline aggregates in slowly-cooled starch solutions prepared by steam jet cooking. *Carbohydrate Polymers*, *48*(2), 161–170, doi:10.1016/S0144-8617(01)00230-2.

Fanta, G. F., Felker, F. C., Shogren, R. L., Byars, J. A., & Salch, J. H. (2005). Crystalline particles formed in slowly-cooled corn starch dispersions prepared by steam jet cooking. The effect of starch concentration, added oil and rate of cooling. *Carbohydrate Polymers*, *61*(2), 222–230, doi:10.1016/j.carbpol.2005.05.013.

Fanta, G. F., Felker, F. C., Shogren, R. L., & Salch, J. H. (2006). Effect of fatty acid structure on the morphology of spherulites formed from jet cooked mixtures of fatty acids and defatted corn starch. *Carbohydrate Polymers*, *66*(1), 60–70, doi:10.1016/j.carbpol.2006.02.017.

Gallant, D. J., Bouchet, B., & Baldwin, P. M. (1997). Microscopy of starch: Evidence of a new level of granule organization. *Carbohydrate Polymers*, *32*, 177–191, doi:10.1016/S0144-8617(97)00008-8.

Granasy, L. (2006). Phase field theory of crystal nucleation and polycrystalline growth: A review. *Journal of Materials Research*, *21*(2), 309–319, doi:10.1557/JMR.2006.0011.

Granasy, L., Pusztai, T., Tegze, G., Warren, J. A., & Douglas, J. F. (2005). Growth and form of spherulites. *Physical Review E (Statistical, Nonlinear, and Soft Matter Physics)*, *72*(1), 011605-011601–011605-011615. doi:10.1103/PhysRevE.72.011605.

Hizukuri, S. (1985). Relationship between the distribution of the chain length of amylopectin and the crystalline structure of starch granules. *Carbohydrate Research*, *141*(2), 295–306, doi:10.1016/S0008-6215(00)90461-0.

Ivanov, D. A., & Magonov, S. N. (2003). Atomic force microscopy studies of semicrystalline polymers at variable temperatures. In G. Reiter, & J. U. Sommer (Eds.), *Polymer crystallization. Observations, concepts and interpretations* (pp. 98–130). Berlin: Springer, doi:10.1007/3-540-45851-4.

Jayakannan, M., & Ramakrishnan, S. (1999). Effect of branching on the crystallization kinetics of poly(ethylene terephthalate). *Journal of Applied Polymer Science*, *74*, 59–66, doi:10.1002/(SICI)1097-4628(19991003)74:1<59::AID-APP6>3.0.CO;2-0.

Jenkins, P. J., Cameron, R. E., & Donald, A. M. (1993). A universal feature in the structure of starch granules from different botanical sources. *Starch/Stärke*, *45*(12), S417–S420, doi:10. 1002/star. 19930451202.

Jenkins, P. J., & Donald, A. M. (1995). The influence of amylose on starch granule structure. *International Journal of Biological Macromolecules*, *17*(6), 315–321, doi:10.1016/0141-8130(96)81838-1.

Khoury, F., & Passaglia, E. (1976). The morphology of crystalline synthetic polymers. In N. B. Hannay (Ed.), *Treatise on solid state chemistry. Crystalline and noncrystalline solids* (pp. 335–496). New York: Plenum Press.

Klucinec, J. D., & Thompson, D. B. (1998). Fractionation of high-amylose maize starches by differential alcohol precipitation and chromatography of the fractions. *Cereal Chemistry*, *75*(6), 887–896, doi:10.1094/CCHEM.1998.75.6.887.

Klucinec, J. D., & Thompson, D. B. (2002). Structure of amylopectins from *ae*-containing maize starches. *Cereal Chemistry*, *79*(1), 19–23, doi:10.1094/CCHEM.2002.79.1.19.

Li, L., Chan, C.-M., Yeung, K. L., Li, J.-X., Ng, K.-M., & Lei, Y. (2000). Direct observation of growth of lamellae and spherulites of a semicrystalline polymer by AFM. *Macromolecules*, *34*(2), 316–325, doi:10.1021/ma000273e.

Nishiyama, Y., Putaux, J.-L., Montesanti, N., Hazemann, J.-L., & Rochas, C. (2010). B→A Allomorphic transition in native starch and amylose spherocrystals monitored by in situ synchrotron X-ray diffraction. *Biomacromolecules*, *11*, 76–87, doi:10.1021/bm900920t.

Nordmark, T. S., & Ziegler, G. R. (2002a). Spherulitic crystallization of gelatinized maize starch and its fractions. *Carbohydrate Polymers*, *49*(4), 439–448, doi:10.1016/S0144-8617(01)00353-8.

Nordmark, T. S., & Ziegler, G. R. (2002b). Structural features of non-granular spherulitic maize starch. *Carbohydrate Research*, *337*(16), 1467–1475, doi:10.1016/S0008-6215(02)00192-1.

Ohtani, T., Yoshino, T., Hagiwara, S., & Maekawa, T. (2000). High-resolution imaging of starch granule structure using atomic force microscopy. *Starch/Stärke*, *52*(5), 150–153, doi:10.1002/1521-379X(200006)52:5<150::AID-STAR150>3.0.CO;2-F.

Peterson, S. C., Fanta, G. F., Adlof, R. O., & Felker, F. C. (2005). Identification of complexed native lipids in crystalline aggregates formed from jet cooked corn starch. *Carbohydrate Polymers*, *61*(2), 162–167, doi:10.1016/j.carbpol.2005.04.012.

Phillips, P. J. (1994). Spherulitic crystallization in macromolecules. In D. T. J. Hurle (Ed.), *Handbook of crystal growth* (pp. 1167–1216). Amsterdam: Elsevier Science B.V.

Planchot, V., Colonna, P., Gallant, D. J., & Bouchet, B. (1995). Extensive degradation of native starch granules by alpha-amylase from *Aspergillus fumigatus*. *Journal of Cereal Science*, *21*(2), 163–171, doi:10.1016/0733-5210(95)90032-2.

Ridout, M. J., Parker, M. L., Hedley, C. L., Bogracheva, T. Y., & Morris, V. J. (2003). Atomic force microscopy of pea starch granules: Granule architecture of wild-type parent, r and rb single mutants, and the rrb double mutant. *Carbohydrate Research*, *338*(20), 2135–2147, doi:10.1016/S0008-6215(03)00309-4.

Ridout, M. J., Parker, M. L., Hedley, C. L., Bogracheva, T. Y., & Morris, V. J. (2004). Atomic force microscopy of pea starch: Origins of image contrast. *Biomacromolecules*, *5*(4), 1519–1527, doi:10.1021/bm0499280.

Ridout, M. J., Parker, M. L., Hedley, C. L., Bogracheva, T. Y., & Morris, V. J. (2006). Atomic force microscopy of pea starch: Granule architecture of the rug3-a, rug4-b, rug5-a and lam-c mutants. *Carbohydrate Polymers*, *65*(1), 64–74, doi:10.1016/j.carbpol.2005.12.016.

Shogren, R. L., Fanta, G. F., & Felker, F. C. (2006). X-ray diffraction study of crystal transformations in spherulitic amylose/lipid complexes from jet-cooked starch. *Carbohydrate Polymers*, *64*(3), 444–451, doi:10.1016/j.carbpol.2005.12.018.

Strobl, G. (2000). From the melt via mesomorphic and granular crystalline layers to lamellar crystallites: A major route followed in polymer crystallization? *The European Physical Journal E*, *3*, 165–183, doi:10.1007/s101890070030.

Strobl, G. (2006). Crystallization and melting of bulk polymers: New observations, conclusions and a thermodynamic scheme. *Progress in Polymer Science*, *31*(4), 398–442, doi:10.1016/j.progpolymsci.2006.01.001.

Sujka, M., & Jamroz, J. (2009). [alpha]-Amylolysis of native potato and corn starches – SEM AFM, nitrogen and iodine sorption investigations. *LWT – Food Science and Technology*, *42*(7), 1219–1224, doi:10.1016/j.lwt.2009.01.016.

Suwanayuen, N. (2009). Degradation of starch spherulites by α-amylase. *Food science* [MSc Thesis] (p. 116). The Pennsylvania State University, University Park.

Szymonska, J., & Krok, F. (2003). Potato starch granule nanostructure studied by high resolution non-contact AFM. *International Journal of Biological Macromolecules*, *33*(1–3), 1–7, doi:10.1016/S0141-8130(03)00056-4.

Ziegler, G. R., Creek, J. A., & Runt, J. (2005). Spherulitic crystallization in starch as a model for starch granule initiation. *Biomacromolecules*, *6*(3), 1547–1554, doi:10.1021/bm049214p.

Ziegler, G. R., Nordmark, T. S., & Woodling, S. E. (2003). Spherulitic crystallization of starch: Influence of botanical origin and extent of thermal treatment. *Food Hydrocolloids*, *17*(4), 487–494, doi:10.1016/S0268-005X(03)00020-1.